New perspective on the scalar meson puzzle, from spontaneous chiral symmetry breaking beyond BCS

Pedro J. de A. Bicudo
Departamento de Física and Centro de Física das Interacções Fundamentais, Edifício Ciência, Instituto Superior Técnico, Avenida Rovisco Pais, 1096 Lisboa, Portugal

(Received 5 February 1998; revised manuscript received 15 January 1999; published 12 August 1999)

We introduce coupled channels of ladder Bethe-Salpeter mesons both in the bound state equation for mesons and in the mass gap equation for chiral symmetry. Consistency is insured by the Ward identities for axial currents, which preserve the Goldstone boson nature of the pion and prevent a systematic shift of the hadron spectrum. We study the decay of a scalar meson coupled to a pair of pseudoscalars. We also show that coupled channels reduce the breaking of chiral symmetry, with the same Feynman diagrams that appear in the coupling of a scalar meson to a pair of pseudoscalar mesons. Exact calculations are performed in a particular confining quark model, where we find that the ground state $I=0$, $^3P_0$ $q\bar{q}$ meson is the $f_0(980)$ with a partial decay width of 40 MeV. We also find a 30% reduction of the chiral condensate due to coupled channels. [S0556-2813(99)00809-2]

PACS number(s): 12.39.Fe, 11.30.Rd, 14.40.Cs, 13.25.Jx

I. INTRODUCTION

The scalar puzzle. The scalar mesons form perhaps the most puzzling family in hadronic physics. The first puzzling fact concerns the experimental errors in the partial decay widths, the decay widths, and even the masses. The lightest scalar $f_0(400-1200)$ has a poorly determined mass. The confidence in the decay widths of the $f_0(980)$ and $a_0(980)$ has also decreased [1] strongly since 1994.

The other puzzling argument concerns the matching of the nine observed states with simple $SU(3)_f$ $q\bar{q}$ states. One would expect four different towers of states built upon the two $I=0$ f_0 (which are not degenerate, for instance because the quark *s* has a clearly larger mass than the quarks *u*, *d*) and to the $I=1$ a_0, and the $I=1/2$ K_0^*. A short glance at Fig. 1 is sufficient to discard the single light and extremely broad state, the $f_0(400-1200)$ as a simple member of this family. Then for the ground states we could ascribe the narrowest states which are, respectively, the $a_0(980)$, $K_0^*(1430)$, $f_0(980)$, and $f_0(1500)$, and for the radial excited states we could, respectively ascribe the $a_0(1450)$, $K_0^*(1950)$, $f_0(1370)$, and $f_0(2200)$. However, the decay widths Γ of the ground state scalars are narrower than expected, when compared with other resonances decaying in the same pseudoscalar pairs but with higher angular momentum, except for the only precisely measured one, the $K_0^*(1430)$. Moreover the breaking of $SU(3)_f$ due to the $m_s > m_u \simeq m_d$ mass difference is nearly double that expected when compared with the vector meson family and with most baryons. The scalar $SU(3)_f$ breaking is only comparable with the splittings in the pseudoscalar family.

The scalar family is also the most interesting place to search for the lightest (*S* wave) non-$q\bar{q}$ states. There are several theoretical candidates to extra states which may be found. The lightest glueball, which is expected from QCD, should be a scalar [2]. The model of Isgur and Weinstein [3] suggests that the narrowest scalars are meson-meson molecules. The one meson exchange potential models for the *NN* interaction usually postulates a scalar meson σ with a light $M \simeq 0.5$ GeV. In strongly coupled effective meson models [4, 5], extra poles appear in the *S* matrix when couplings are large. These meson models turn out to be the most successful models so far, explaining with complex nonlinear effects not only the narrow $a_0(980)$ and $f_0(980)$ which are due to the vicinity of the *KK* threshold, but also the very wide and light $f_0(400-1200)$.

The relevance of chiral symmetry breaking. Chiral symmetry breaking is important for the study of scalar mesons and their decays for several reasons. Unlike the vector, axial, and tensor mesons, the scalar and pseudoscalar mesons are mixed by the chiral rotations

$$\bar{\psi}\psi \rightarrow \cos(\theta)\bar{\psi}\psi + i\sin(\theta)\bar{\psi}\gamma_5\psi,$$
$$\bar{\psi}\gamma_5\psi \rightarrow -i\sin(\theta)\bar{\psi}\psi + \cos(\theta)\bar{\psi}\gamma_5\psi, \quad (1)$$

thus scalars and pseudoscalars are particularly sensitive to the chiral symmetry. The very small mass of the pseudoscalars is usually explained with chiral symmetry breaking.

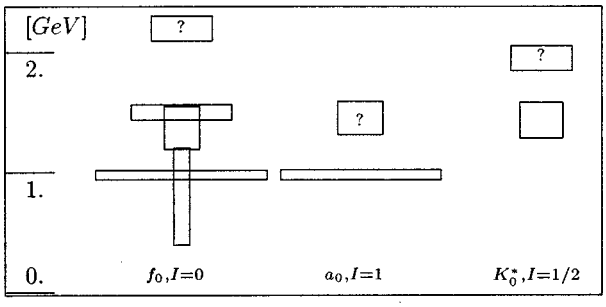

FIG. 1. We represent with rectangles the experimentally observed scalar resonances according to the Review of Particle Properties, and mark the unconfirmed ones with a question mark. The height of each rectangle is equal to the decay width Γ of the resonance. In a naive quark model, the a_0 and K_0^* channels should show half of the resonances of the f_0 channel.

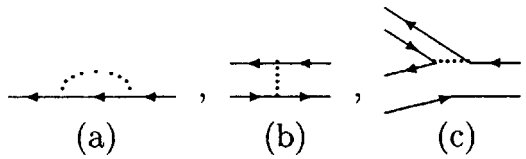

FIG. 2. We show the quartic diagrams which may contribute to the bound state equation. In the strong coupling BCS, (a) is included in the self-energy and (b) is included in the interaction kernel. Diagram (c) which creates or annihilates quark-antiquark pairs is only used in what we call beyond BCS.

Moreover, since scalars decay essentially in pseudoscalars, the pseudoscalar mass is important for the scalar decay. Thus we expect that not only the pseudoscalar mesons but also the scalars must contain the signature of the breaking of chiral symmetry. On the other hand, the breaking of chiral symmetry is generated from the trivial vacuum by scalar condensation, and we also expect that the scalar properties should affect the breaking of chiral symmetry.

These effects have been studied in phenomenological meson sigma models, see, for instance Ref. [5]. At the more microscopic level of quarks, dynamical spontaneous chiral symmetry breaking (χSB) has been worked out in the past with several different quark-quark effective interactions, at the same level as Bardeen, Cooper, and Schrieffer (BCS) did for superconductivity [6]. Since Nambu and Jona-Lasinio (NJL) [7] and until recently [8,9] the mass gap equation in chiral physics has been so far of the BCS type [7], including only the first order contribution from the quark-quark interaction. In this case the quark condensate consists of scalar $^3P_0$ quark antiquark pairs [10]. At the BCS level, which is very consistent, it is possible to derive the mass gap equation in several different but equivalent methods. The pseudoscalar meson properties have been studied in great detail and the full meson spectrum has been also been calculated in the literature [11]. However the BCS approach is not exact in the case where coupled channels of mesons are included.

Coupled channels of mesonic $q\bar{q}$ pairs. In the case of weak coupled channel effects, it should be acceptable to start from bound states obtained at the BCS level and couple them with the help of the annihilation diagrams of Fig. 2, without changing the mass gap equation. In this sense we started some years ago to develop a program [12] to study coupled channel effects in quark models with chiral symmetry breaking.

The first result of our program was to reproduce [12] at the BCS level the strong decay of the vector meson ρ (and of the ϕ). These decays have been studied with other methods recently [14]. Later we extended our program to the nucleon interactions and had good results [12] in the *KN* *s*-wave scattering, the $F_{N\pi N}$ and $F_{N\pi\Delta}$ derivative couplings and the *NN* short range interaction [13].

However, there is a recent trend in the literature to reevaluate coupled channel effects in hadronic phenomena. Some years ago they were not supposed to account for more than 10% of a hadron mass but presently they are supposed to contribute with a negative mass shift of the order of 50% of the bare mass [15–17].

Moreover it is possible to prove that the vacuum solution

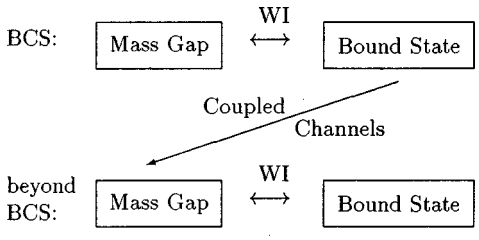

FIG. 3. We illustrate the principle which is followed in this paper to include the coupled channels in the mass gap equation.

of the BCS mass gap equation is not exact when coupled channels are included. Suppose that the mass gap equation for chiral symmetry breaking was solved at the BCS level, i.e., without including the coupled channels, then a bare pion with vanishing bare mass would be found. If the coupled channels were then included, *a posteriori*, in the bound state equation then the pion mass would be the sum of the small bare mass plus a mass shift and thus would have a resulting nonvanishing mass, which implies that the pion lost its Goldstone boson nature. This result is unavoidable, and can be proved variationally. Thus the mass gap should be solved beyond BCS, especially when scalar mesons are studied.

Solving this problem is a cornerstone of our program. It amounts to joining the BCS mechanism with the mean field expansion of effective mesons. The logical path of the method we will follow is illustrated in Fig. 3. Self-consistency is insured by Ward identities, and the scalar-pseudoscalar coupling will turn out to be crucial for this development. The reward of solving chiral symmetry breaking with coupled channels is a π with a vanishing positive mass in the chiral limit complying with all the theorems of PCAC, and a tower of resonances (including the scalar meson resonances) above the π with higher masses due to radial, angular, or spin excitations. In particular the resonances also have an imaginary component of the mass $-i\Gamma/2$ that describes the decay width into the open channels.

The paper. The aim of this paper is to study at the quark level some meson decays which have been studied in the literature without including directly the full microscopic quark contributions [4,5]. We specialize in the ground state $f_0 \to \pi\pi$ decay. We also study the effect of the meson coupled channels on the quark condensed vacuum.

The remainder of this paper is organized as follows. In Sec. II we review the scalar masses and decays at the BCS level. This includes the choice of an effective interaction for quarks, the mass gap equation and the Bethe-Salpeter equation at the BCS level, the scalar coupling to pseudoscalars, and the scalar decays width. In Sec. III we produce a finite extension beyond BCS for a class of confining effective interactions, derive the mass gap equation with coupled channels, link it to the scalar-pseudoscalars coupling, and solve the mass gap equation. Results are shown in Sec. IV together with their discussion. We also include four Appendixes.

II. THE BCS LEVEL FOR A PARTICULAR FORMALISM

A. The choice of an effective interaction

The quantitative results of this paper will be obtained with a particular chiral invariant strong potential which is an ex-

tended version of the NJL potential [7]. For the study of dynamical χSB it is crucial to have a closed chiral invariant model where calculations can be carried until the end, because precise cancellations occur. A result of this constraint is that the same interaction must be used in the kernel of the bound state equation and in the creation of quark-antiquark pairs. Another result concerns two-body scalar interactions which are ruled out in this scheme because they violate chiral symmetry.

Recently it has been found that this potential can be linked to QCD [18]. We first integrate formally the gluons from the QCD action, and get an action of Dirac quarks which interact via cumulants of gluons. Expanding in cumulants we get the Hamiltonian

$$H=\int d^3x\Big[\psi^\dagger(x)(m_0\beta-i\vec{\alpha}\cdot\vec{\nabla})\psi(x) + \frac{1}{2}g^2\int d^4y\,\overline{\psi}(x)\gamma^\mu\frac{\lambda^a}{2}\psi(x) \times\langle A^a_\mu(x)A^b_\nu(y)\rangle\overline{\psi}(y)\gamma^\nu\frac{\lambda^b}{2}\psi(y)+\cdots. \quad (2)$$

The first cumulant, of two gluons, can be evaluated in the modified coordinate gauge,

$$\langle A^a_\mu(x)A^b_\nu(y)\rangle=x^k y^l\int_0^1 d\alpha d\beta\alpha^{n(\mu)}\beta^{n(\nu)} \times\langle F^a_{k\mu}(x_0,\alpha\mathbf{x})F^b_{l\nu}(y_0,\beta\mathbf{y})\rangle \quad (3)$$

as a function of the nonlocal gluon condensate. The calculation on the lattice [19] of the full nonlocal gluon correlator lends support [18] for the picture of a simplified Dirac quark-quark interaction

$$g^2\langle A^a_\mu(x)A^b_\nu(y)\rangle\simeq-\frac{3}{4}\delta_{ab}g_{\mu\nu}\{g_{\mu 0}[K_0^3(\mathbf{x}-\mathbf{y})^2-U] + a g_{\mu i}k_0^3(\mathbf{x}-\mathbf{y})^2\}\delta(x^0-y^0). \quad (4)$$

Because the Gell-Mann matrices are traceless there will be no tadpoles in this scheme. This interaction belongs to a class of extended NJL models, which has the single drawback of using an instantaneous potential (except for Lorentz invariant extensions [20] of this class). But it has the advantage of being confining which allows one to study the whole [11,12,21–25] hadron spectrum. For the theoretical foundations of these models, including the connection to both pertubative and nonpertubative QCD, see Ref. [26].

This particular simple model is in very good agreement with the experiments: hadronic spectroscopy, the decays of the vector mesons ρ and Φ, the coupling of a π to a N or Δ and the NN short range interaction [12]. Moreover it suggests that chiral symmetry breaking is very stable in the presence of nuclear matter [25]. While confinement is an essential physical aspect of the model, the instantaneous approximation simplifies drastically the energy dependence of the interaction, and allows us to work in a framework which is familiar to Schrödinger's equations.

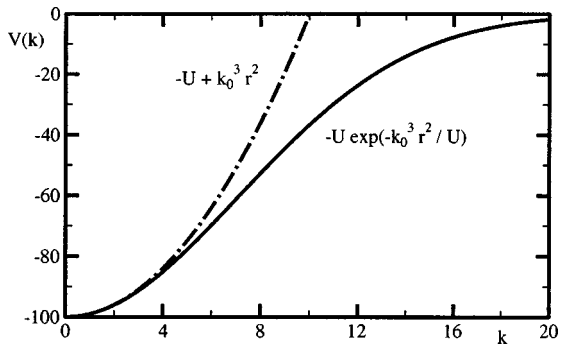

FIG. 4. $-Ue^{-K_0^3r^2/U}$ is an example of a potential which tends to $-U+K_0^3r^2$ in the limit of infinite U. We illustrate this in the case where $K_0=1$, $U=100$.

Another class of extended NJL interactions is Euclidean, and, due to the structure of the interaction, usually has no analytic continuation to the Minkowsky space and lacks confinement. This class has been extended in many different directions. For instance, finite size bound states were included with the global color model of Ref. [27], and a sophisticated interaction with a general tensor structure, an almost linear long range, and a pertubative short range is found in Ref. [28].

The Fourier transform of the potential (4) is

$$\Omega_l V_l(k)\otimes\Omega_l=\frac{-3}{4}\frac{\vec{\lambda}}{2}\otimes\frac{\vec{\lambda}}{2}[\gamma_0\otimes\gamma_0(-K_0^3\Delta_k-U) + a\vec{\gamma}\otimes\vec{\gamma}(-K_0^3\Delta_k)](2\pi)^3\delta^3(k), \quad (5)$$

where we do not display the sum in color and Dirac indices. In Eq. (5) the operators Ω_l include both the color Gell-Mann matrices and the Dirac matrices. The factor $-\frac{3}{4}$ simplifies the color contribution for color singlets.

The $\gamma_0\cdot\gamma_0$ term in the potential is the limit of a series of attractive potentials, see Fig. 4, and U is an arbitrarily large infrared constant. The infinite U reappears in the self-energy and in color singlet channels this cancels the infinitely attractive potential. Any colored state will have a mass proportional to U and in this sense will be confined, see Appendix A.

The choice of a harmonic potential is not crucial, a linear [22] or funnel potential has also been used, but a quadratic form is simpler. In the case of light quarks the current quark mass m_0 is almost vanishing and it essentially affects the family of the π which is a quasi-Goldstone boson.

The $\vec{\gamma}\cdot\vec{\gamma}$ term improves the Lorentz invariance of the wave function of pions which must be relativistic in the scalar decay. Clearly the wrong result of a simple $\gamma_0\gamma_0$ instantaneous interaction is the constant f_π which is quite small and is not Lorentz invariant, $f_\pi^{(s)}\neq f_\pi^{(t)}$. The hope to cure f_π with covariant extensions of the model turned out to fail since they merely [20] increased f_π by 30%. The value for the parameter a which renders the f_π Lorentz invariant is $a=-0.18$, and for most calculations (except for f_π which is

increased by 300%, see Sec. II D) this a yields a result comparable to the one we had for $a=0$. The small a suggests that the cure of f_π may be related with a pertubative short range [26] quark-quark interaction.

Once a is fixed, this model has the single scale of the oscillator parameter K_0. The simplest dimensionless units of $K_0=1$ will be used from now on in computations. When comparing with experiments we will rescale K_0 to the value of $K_0=330\,\mathrm{MeV}$ which gives the best overall fit of the meson spectrum. In the case of $a=0$ the the full light quark meson spectrum was well fitted [11] with $K_0=290\,\mathrm{MeV}$. In the case of a finite a the quark-antiquark interaction is weaker, and a slight rescaling of K_0 is needed.

B. Chiral symmetry breaking at the BCS level with quarks and antiquarks

At the BCS level and with a color dependent interaction the Schwinger-Dyson equation for the quark self-energy (which is also the mass gap equation) is

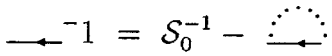

$$\mathcal{S}^{-1}=-i\not{p}-\Sigma \tag{6}$$

where the full (up to the approximation which is chosen) propagator $\mathcal{S}$ is denoted as usual by an arrowhead on a line. The subindex $_0$ is reserved for the free functions. The effective quark-quark two-body interaction of Eq. (2), a chiral invariant and color dependent interaction, is represented with a dotted line. The Bethe-Salpeter equation for the vertex is related by the Ward identities with Eq. (6), see Appendix C,

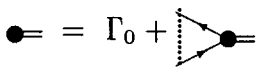

$$\Gamma(p,q)=\Gamma_0+\int\frac{d^4k}{(2\pi)^4}V(k)\Omega S(p+k)\,\Gamma(p+k,q+k)S(q+k)\Omega \tag{7}$$

where the full vertex Γ^μ is denoted by a filled circle with two emerging lines. When Eq. (7) is iterated, we find that it includes the Bethe-Salpeter ladder, which will be represented diagrammatically by a box with 4 emerging lines,

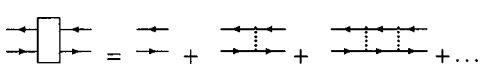

(8)

where the ladder represents the mesons, see Appendix C. In this way the quark propagator, the vertices and the mesons are intertwined.

In this case of an instantaneous interaction, it is convenient to express the Dirac fermions in terms of Weyl fermions, in order to find the hadron spectrum. The Dirac propagator can be decomposed in a quark propagator and an antiquark propagator, moving both forward in time.

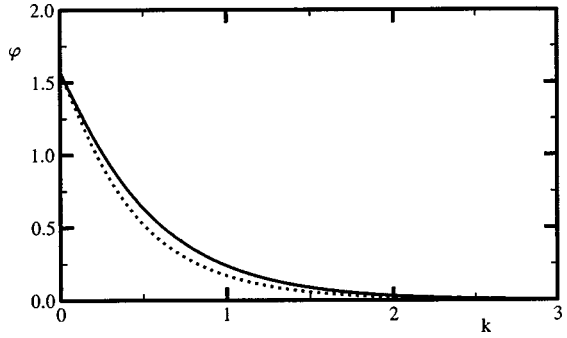

FIG. 5. We show the BCS chiral angle $\varphi(k)$ in units of $K_0=1$. We also represent with a dotted line the chiral angle that we obtain going beyond BCS.

$$\mathcal{S}_{\mathrm{Dirac}}(K_0,\vec{k})=\frac{i}{\not{k}-m+i\epsilon}=\frac{i}{K_0-E+i\epsilon}\frac{1+(m/E)\beta+(k/E)\vec{\alpha}\cdot\hat{k}}{2}\beta-\frac{i}{-K_0-E+i\epsilon}\frac{1-(m/E)\beta-(k/E)\vec{\alpha}\cdot\hat{k}}{2}\beta. \tag{9}$$

It is convenient to use [11,10] the quark energy projectors

$$\Lambda^+=\frac{1}{2}(1+S\beta+C\hat{k}\cdot\vec{\alpha})=\sum_s u_s u_s^\dagger,$$

$$\Lambda^-=\frac{1}{2}(1-S\beta-C\hat{k}\cdot\vec{\alpha})=\sum_s v_s v_s^\dagger, \tag{10}$$

where $S=\sin(\varphi)=m/E$, $C=\cos(\varphi)=k/E$ and φ is a chiral angle, which in the non condensed case is equal to arctan (m_0/k) (m_0 is the current mass of the quark), but is not determined from the onset when chiral symmetry breaking occurs. In this case the physical quark mass is a variational function $m=m(k)$ which is determined by the mass gap equation. This is equivalent to using the chiral angle $\varphi=\varphi(k)$ as the variational function. In Fig. 5 we show examples of nontrivial solutions for the function $\varphi(k)$.

The energy projectors can be decomposed in the quark spinor $u(k)$ and in the antiquark spinor $v(k)$:

$$u_s(\mathbf{k})=\frac{\Lambda^-}{\sqrt{(1+S)/2}}u_s(0)=\left[\sqrt{\frac{1+S}{2}}+\sqrt{\frac{1-S}{2}}\hat{k}\cdot\vec{\alpha}\right]u_s(0),$$

$$v_s(\mathbf{k})=\frac{\Lambda^-}{\sqrt{(1+S)/2}}v_s(0)=\left[\sqrt{\frac{1+S}{2}}-\sqrt{\frac{1-S}{2}}\hat{k}\cdot\vec{\alpha}\right]v_s(0)=-i\sigma_2\gamma_5 u_s^*(\mathbf{k}). \tag{11}$$

And finally the Dirac quark propagator is decomposed as

$$\mathcal{S}_{\rm Dirac}(w,\vec{k}) = u(k)\mathcal{S}_q(p_0,\vec{k})u^\dagger(k)\beta - v^\dagger(k) \times \mathcal{S}_{\bar{q}}(-p_0,-\vec{k})v(k)\beta, \tag{12}$$

where the quark and antiquark Weyl propagators are

$$\mathcal{S}_q(w,\vec{k}) = \mathcal{S}_{\bar{q}}(w,\vec{k}) = \frac{i}{w - E(k) + i\epsilon}. \tag{13}$$

This quark and antiquark formalism is convenient to calculate hadron spectroscopy. With Weyl propagators the BS equation simplifies into the Salpeter equation, in a form which is as close as possible to the more intuitive Schrödinger equation. In the Feynman rules with Weyl propagators, we choose to redefine the vertices of the effective potential which now include the spinors $u^\dagger$, u, $v^\dagger$, and v. The minus sign which affects the antiquark propagator in Eq. (12) could also be included in the vertices with $v^\dagger$, but we prefer to recover the equivalent rules which are common to nonrelativistic field theory. This minus sign, together with the one from the fermion loops will be included in the antiquark vertex and in diagrams with quark exchange or with antiquark exchange. The Dirac vertex γ_0 is now replaced by $u^\dagger u$, $u^\dagger v$, $v^\dagger u$, or $-v^\dagger v$ as the vertex is respectively connected to a quark, a pair creation, a pair annihilation, or an antiquark; and the Dirac vertex $\vec{\gamma}$ is, respectively, replaced by $u^\dagger\vec{\alpha}u$, $u^\dagger\vec{\alpha}v$, $v^\dagger\vec{\alpha}u$, or $-v^\dagger\vec{\alpha}v$. We choose the graphical notation for the Weyl propagators of quarks and antiquarks,

$$\mathcal{S}_{\rm Dirac}(w,\vec{k}) = \overset{w,\vec{k}}{\longleftarrow} D \quad ,$$

$$\mathcal{S}_q(w,\vec{k}) = \overset{w,\vec{k}}{\longleftarrow} \quad , \quad \mathcal{S}_{\bar{q}}(-w,-\vec{k}) = \overset{w,\vec{k}}{\longrightarrow} \tag{14}$$

where the diagrams using the Feynman rules corresponding to the Dirac fermion propagators will have a subindex $_{\rm D}$ in the remaining of the paper. In the case of the Weyl propagators (which will be used more often the the Dirac propagators) the quark will be represented with an arrow pointing to the left while the arrow pointing to the right represents an antiquark (both move forward in the time direction).

C. The BCS mass gap equation and the quark energy

Here we derive the mass gap equation, and the quark dispersion relation, replacing the propagator of Eq. (12) in the Schwinger-Dyson equation for the quark self-energy (6),

$$u \overset{w,\vec{k}}{\longleftarrow}{}^{-1} u^\dagger - v \overset{w,\vec{k}}{\longrightarrow}{}^{-1} v^\dagger = \beta\frac{\not{k} - m_0}{i} - \beta \overset{\cdots}{\longleftarrow} D \tag{15}$$

Another equivalent method is to use the Hamiltonian formalism for the quark and antiquark creators and annihilators [10], and find the Bogoliubov-Valatin transformation which would minimize the vacuum energy density. In that Hamiltonian formalism the mass gap equation is also obtained when the quark antiquark pair creation operators are postulated to vanish in the Hamiltonian, in order to ensure the vacuum stability against spontaneous generation of scalars. With the present method we project Eq. (15) with the spinors $u^\dagger\ldots u$ and $u^\dagger\ldots v$, and we get directly the quark and antiquark energy and the mass gap equation

$$E(k) = u_s^\dagger(k)\left\{k\hat{k}\cdot\vec{\alpha} + m_0\beta - \int\frac{dw'}{2\pi}\frac{d^3k'}{(2\pi)^3}iV_l(k-k') \times\left[\frac{\Omega_l\Lambda^+(k')\Omega_l}{w' - E(k') + i\epsilon} - \frac{\Omega_l\Lambda^-(k')\Omega_l}{-w' - E'(k') + i\epsilon}\right]\right\}u_s(k),$$

$$0 = u_s^\dagger(k)\left\{k\hat{k}\cdot\vec{\alpha} + m_0\beta - \int\frac{dw'}{2\pi}\frac{d^3k'}{(2\pi)^3}iV(k-k') \times\left[\frac{\Omega_l\Lambda^+(k')\Omega_l}{w' - E(k') + i\epsilon} - \frac{\Omega_l\Lambda^{-1}(k')\Omega_l}{-w' - E(k') + i\epsilon}\right]\right\}v_{s''}(k). \tag{16}$$

In the case of an instantaneous interaction, the loop integral in the energy w removes the pole in the propagator

$$\int\frac{dw}{2\pi}\frac{i}{w - E(k) + i\epsilon} = \frac{1}{2} \tag{17}$$

and in the case of a quadratic interaction, the loop integral in the momentum is transformed in a Laplacian, see Eq. (5). Some useful properties are

$$u_s^\dagger u_{s'} = 1\,\delta_{ss'}, \quad u_s^\dagger v_{s'} = 0[\vec{\sigma}\cdot\hat{k}i\sigma_2]_{ss'},$$

$$u_s^\dagger\beta u_{s'} = S\,\delta_{ss'}, \quad u_s^\dagger\beta v_{s'} = -C[\vec{\sigma}\cdot\hat{k}i\sigma_2]_{ss'},$$

$$u_s^\dagger\vec{\alpha}\cdot\hat{k}u_{s'} = C\,\delta_{ss'}, \quad u_s^\dagger\vec{\alpha}\cdot\hat{k}v_{s'} = S[\vec{\sigma}\cdot\hat{k}i\sigma_2]_{ss'},$$

$$u_s^\dagger\beta\vec{\alpha}\cdot\hat{k}u_{s'} = 0\,\delta_{ss'}, \quad u_s^\dagger\beta\vec{\alpha}\cdot\hat{k}v_{s'} = 1[\vec{\sigma}\cdot\hat{k}i\sigma_2]_{ss'}. \tag{18}$$

We get finally for the quark energy,

$$E(k) = kC + m_0 + \frac{1}{2}[+S\Delta(S) + C\hat{k}\cdot\Delta(\hat{k}C)] + \frac{U}{2} + a\frac{1}{2}[-3S\Delta(S) - C\hat{k}\cdot\Delta(\hat{k}C)] = \frac{U}{2} + kC + m_0S - \frac{\dot{\varphi}^2}{2} - \frac{C^2}{k^2} - a\left[SC\Delta\varphi - \frac{C^2}{k^2} - \left(S^2 + \frac{1}{2}\right)\dot{\varphi}^2\right], \tag{19}$$

where in color singlets the $U/2$ term will cancel the $-U$ term from the two-body quark potential. For the mass gap equation we get

$$0=\left\{kS-m_0C+\frac{1}{2}[-C\Delta(S)+S\hat{k}\cdot\Delta(\hat{k}C)]\right.$$
$$\left.+a\frac{1}{2}[+3C\Delta(S)-S\hat{k}\cdot\Delta(\hat{k}C)]\right\}[\vec{\sigma}\cdot\hat{k}i\sigma_2]_{ss'}$$
$$=-\Delta\varphi+2kS-2m_0C-\frac{2SC}{k^2}-a\left[-(2C^2+1)\Delta\varphi\right.$$
$$\left.+2SCV\left(\dot{\varphi}^2-\frac{1}{k^2}\right)\right]. \quad (20)$$

The mass gap equation is in general a nonlinear integral equation, but in this case of a harmonic potential it simplifies to a differential equation. We solve it numerically with the Runge-Kutta and shooting method, see Fig. 5 for the solution.

D. The pseudoscalar and scalar solutions to the Salpeter equation

The homogeneous Salpeter equation for a meson (a color singlet quark-antiquark bound state) is, according to Appendix C,

$$\frac{+M(P)-E(k_1)-E(k_2)}{i}\phi^+(k,P)$$
$$=-iu^\dagger(k_1)\chi(k,P)v(k_2),$$
$$\frac{-M(P)-E(k_1)-E(k_2)}{i}\phi^{-t}(k,P)$$
$$=-iv^\dagger(k_1)\chi(k,P)u(k_2),$$

$$\chi(k,P)=\int\frac{d^3k'}{(2\pi)^3}V_l(k-k')\Omega_l[u(k_1')\phi^+(k',P)v^\dagger(k_2')$$
$$+v(k_1')\phi^{-t}(k',P)u^\dagger(k_2')]\Omega_l, \quad (21)$$

where $k_1=k+P/2$, $k_2=k-P/2$, and P is the total momentum of the meson. We use the Bethe-Salpeter amplitude χ as an intermediate step to compute the contribution of interaction V to the bound state equation. The wave functions ϕ^+ and ϕ^- are equivalent to the Bethe-Salpeter amplitude χ. For color singlets the contribution of the infinite infrared constant U are canceled, see Appendix A. The equation is also flavor independent, and we will now concentrate on the momentum⊗spin part of the wave functions. We will now drop the U term, the color matrices and the color dependence from the equations. In this section the matrices Ω_l will only include the Dirac structure $\Omega_l\otimes\Omega_l=\gamma_0\otimes\gamma_0+a\vec{\gamma}\cdot\otimes\vec{\gamma}$. With the aim of studying the f_0 decay in a pair of π, we will now solve the bound state equation equation for the scalar f_0 in its center of mass frame and the equation for the pseudoscalar ground state π in the limit of small P and in the limit of large P.

Due to the large mass of the scalar meson f_0 in this model, it turns out that the negative energy ϕ^- component for the ground state is less than 10% of the positive energy component ϕ^+. The Schrödinger limit, where only the positive energy component is considered, is therefore acceptable. A general form for the $^3P_0$ wave function for the scalar is

$$\phi^+(k)_{s_1s_2}=k\phi_s(k)\frac{[\vec{\sigma}\cdot\hat{k}i\sigma_2]_{s_1s_2}}{\sqrt{2}} \quad (22)$$

the truncated BS amplitude is then

$$\chi_s=-\Omega_l\Delta\frac{2k\phi_s(k)}{1+S}\Lambda^+u_{s_1}(0)\frac{[\vec{\sigma}\cdot\hat{k}i\sigma_2]_{s_1s_2}}{\sqrt{2}}v^\dagger_{s_2}(0)\Lambda^-\Omega_l$$
$$=\Omega_l\Delta\frac{\Lambda^+\beta\vec{\alpha}\cdot\vec{k}\phi_s(k)}{\sqrt{2}}\Omega_l. \quad (23)$$

We get for left-hand side of Eq. (21),

$$u^\dagger(k)\chi(k,0)v(k)=\frac{1+a}{2}\Delta(\phi^+)+\frac{1-a}{2}S\Delta(S\phi^+)$$
$$+\frac{1-3a}{2}C\Delta(C\phi^+)+\frac{1-3a}{k^2}C^2\phi^+, \quad (24)$$

and the radial Salpeter equation for the scalar in the center of mass is

$$\left[2E(k)-M-\left(\frac{d^2}{dk^2}-\frac{2}{k^2}-\frac{\dot{\varphi}^2}{2}+\frac{C^2}{k^2}\right)-a\left(-C^2\frac{d^2}{dk^2}\right.\right.$$
$$\left.\left.+2SC\dot{\varphi}\frac{d}{dk}-\frac{C^2}{k^2}+SC\ddot{\varphi}+\frac{1+2C^2}{2}\dot{\varphi}^2\right)\right]k^2\phi_s=0. \quad (25)$$

Solving the bound state equation we find that the solution of the equation is very close to a Gaussian,

$$\phi_s(k)\simeq\frac{e^{-k^2/2\alpha_s^2}}{\mathcal{N}_s},\quad \mathcal{N}_s^{-1}=\frac{4\sqrt{\pi\sqrt{\pi}}}{\sqrt{3}\alpha_s^{5/2}},\quad \alpha_s\simeq0.476 \quad (26)$$

and the mass is $M=2.94\,K_0=970$ MeV which is close to the most probable experimental mass of the f_0 ground state.

We now study the pseudoscalar ground state in the low P limit, which was already studied extensively in the literature [11,12]. For vanishing P we find that $\phi^+=-\phi^-$ and both are proportional to $\sin(\varphi)$. This is due to the Goldstone boson nature of the π, see the result of Appendix C. However, this component of the wave function has zero norm, and it is necessary to include the next order of the expansion in P to determine the norm. The most general low P pseudoscalar wave function is then

$$\phi^+=\mathcal{N}_p^{-1}\left(S+\frac{M(P)}{k}f_1+ig_1\frac{\vec{P}}{k}\cdot\hat{k}\times\vec{\sigma}\right)\frac{i\sigma_2}{\sqrt{2}},$$

$$\phi^-=\mathcal{N}_p^{-1}\left(-S+\frac{M(P)}{k}f_1-ig_1\frac{\vec{P}}{k}\cdot\hat{k}\times\vec{\sigma}\right)\frac{i\sigma_2}{\sqrt{2}}, \quad (27)$$

where the norm is a function of the π energy

$$\mathcal{N}_p^2=(2f_\pi^{(t)})^2M,\quad M^2(P)=M^2(0)+P^2\sqrt{\frac{f_\pi^{(s)}}{f_\pi^{(t)}}},$$

$$M^2(0)=-\frac{2m_0\langle\bar{\psi}\psi\rangle}{f_\pi^{(t)^2}},\quad \langle\bar{\psi}\psi\rangle=-6\int\frac{d^3k}{(2\pi)^3}S \tag{28}$$

and where in the case of an instantaneous interaction there are [11,12] usually two different $f_\pi^{(t)}$ and $f_\pi^{(s)}$,

$$f_\pi^{(t)}=\sqrt{\frac{3}{\pi^2}\int_0^\infty dkkf_1S},$$

$$\sqrt{f_\pi^{(s)}f_\pi^{(t)}}=\sqrt{\frac{1}{2\pi^2}\int_0^\infty dk-k^2S\dot{\varphi}+4kC(g_1+1/2)}. \tag{29}$$

Substituting the wave functions of Eq. (27) in Eq. (21), and expanding the resulting equation up to the first order in P, we get the equations for the f_1 and g_1 components

$$\ddot{f}_1=\frac{1}{1+a(2S^2+1)}[-kS+(2Ck)f_1+4a(-SC\Delta\varphi-C^2k^2+S^2\dot{\varphi}^2+\dot{\varphi}^2/2)f_1-4aSC\dot{\varphi}(\dot{f}_1-f_1/k)], \tag{30}$$

$$\ddot{g}_1=\frac{1}{1+a(2S^2-1)}[kC+(2kC+2S^2/k^2)g_1+2a(S^2/k^2-2SC\Delta\varphi-2S^2\dot{\varphi}^2)g_1-4aSC\dot{\varphi}(\dot{g}_1-g_1/k)]. \tag{31}$$

It turns out that the parameter a has little effect on most functions, except for f_1 (see Fig. 6). The homogeneous equation for f_1 has the solution $a_0=-0.195$ and thus f_1 is proportional to $1/(a-a_0)$. This will essentially affect $f_\pi^{(t)}$, $f_\pi^{(s)}$ and the pion velocity c. We find for $a\simeq-0.18$ that $c=1$, $f_\pi^{(t)}=f_\pi^{(s)}=0.21\,K_0\simeq 69\,\mathrm{MeV}$. This shows a clear improvement of the model, with a correct relativistic pion and a better f_π.

We now discuss the pseudoscalar ground-state in the other limit of large momentum P. In this case the negative energy components are suppressed by a factor of $1/P$. The chiral angle φ, depicted in Fig. 5 vanishes completely, and the spinors are simpler, for instance,

$$u_s(k_1)\simeq\frac{1+\vec{\alpha}\cdot\hat{k}_1}{\sqrt{2}}u_s(0),\quad \hat{k}_1\simeq\hat{P}+\frac{2}{P}\hat{k}_\perp, \tag{32}$$

where the index $\perp$ denotes the projection $\vec{k}-(\vec{k}\cdot\hat{P})\hat{P}$ of a vector $\vec{k}$ in the plane perpendicular to $\vec{P}$. The vertices, up to first order in $1/P$ are, for instance,

$$u_s^\dagger(k_1)u_{s'}(k_1')\simeq\delta_{ss'}-\frac{1}{P}i\vec{\sigma}_{ss'}\hat{P}\times(\hat{k}_\perp-\hat{k}_\perp'),$$

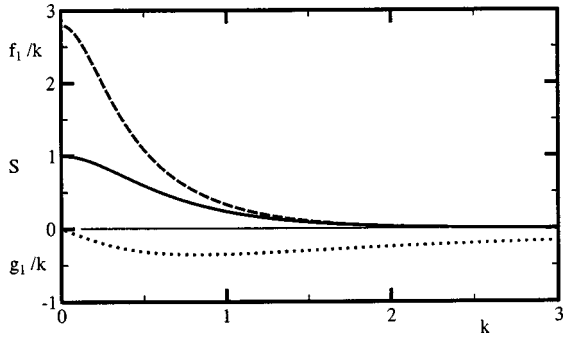

FIG. 6. We represent the π wave functions S, f_1/k, and g_1/k, respectively, with solid, dashed, and dotted lines, in the dimensionless units $K_0=1$.

$$u_s^\dagger(k_1)\vec{\alpha}u_{s'}(k_1')\simeq\hat{P}\,\delta_{ss'}+\frac{(\hat{k}_\perp+\hat{k}_\perp')+i\vec{\sigma}\times(\hat{k}_\perp-\vec{k}_\perp')}{P}. \tag{33}$$

Up to first order in $2/P$ the equation for positive and negative energy bound-state functions $\phi^\pm(k)i\sigma_2/\sqrt{2}$ is

$$0\simeq\left(P+\frac{2k^2}{P}\mp M-(1-a)\Delta_k\right)\phi^\pm(k)-2i(1-a)\frac{\hat{P}}{P}\times\vec{\nabla}_k\cdot\{\vec{\sigma},\phi^\pm(k)\}-a\Delta_k\phi^\mp(k)-\frac{2}{P^2}\vec{\sigma}_\perp\cdot\phi^\mp(k)\vec{\sigma}_\perp. \tag{34}$$

We find that the wave function has a component with structure $i\vec{\sigma}\cdot\hat{P}\times\vec{k}$. However, this component is smaller than the s-wave component by a factor of less than $1/P$. Thus we find that the momentum$\otimes$spin solution in the limit of large P, is essentially a positive energy Gaussian function $\phi_p(k)\times(i\sigma_2/\sqrt{2})$,

$$\phi_p(k)\simeq\frac{e^{-k^2/2\alpha_p^2}}{\mathcal{N}_p},\quad \mathcal{N}_p^{-1}=\left(\frac{2\sqrt{\pi}}{\alpha_p}\right)^{3/2},\quad \alpha_p^2=\sqrt{\frac{1-a}{2}}P. \tag{35}$$

For large momentum P we find that ϕ^+ is quite flat in k, while ϕ^- is almost negligible,

$$\phi^-\simeq\frac{a}{2P}\Delta\phi^+. \tag{36}$$

This result is consistent with relativistic space contraction. We checked that the components that we neglected here would yield a small contribution to the f_0 decay.

E. The coupling of a scalar to a pair of pseudoscalars

The form factor $F(P)$ for the coupling of a scalar f_0 to a pair of π can be decomposed in diagrams where a quark (antiquark) line either emits (absorbs) a pseudoscalar or a scalar. We use the truncated Bethe-Salpeter amplitude χ, as an intermediate step to compute the coupling of a meson to a quark line $u^\dagger\chi u$. $F(P)$ is represented with a large triangle

and the bound state amplitudes χ and ϕ are represented with small triangles,

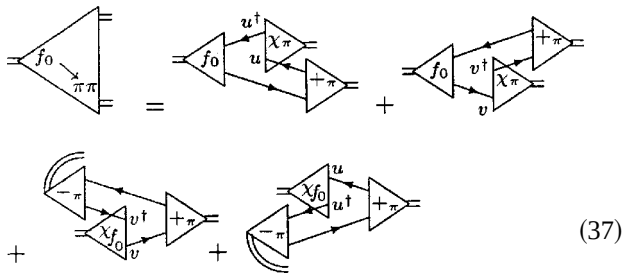

(37)

This includes the $q\bar{q}$ pair creation or annihilation of Fig. 2. The same irreducible interaction for quarks which is used in the bound state equations is also [29] used for the annihilation. In Eq. (37) the loop energies are trivial, see for instance Eq. (A3), and we now compute the momentum⊗spin contribution.

We first consider the limit of a coupling to pions of low momentum P. The coupling of the pseudoscalar to the quark is derivative and thus is suppressed. For instance, in the case of a massless π in the center of mass, using the wave function of Eq. (27), we find that

$$\chi=[-(1-3a)\sqrt{2}\mathcal{N}_p^{-1}\Delta(S)]\beta\gamma_5 + o(P)\Rightarrow u^\dagger(k)\chi(k,0)u(k)=o(P), \tag{38}$$

which is consistent with the derivative coupling of a pion to a quark. The dominant contribution includes the coupling of the $^3P_0$ scalar meson to the quark (antiquark) line. The coupling $F(P)$ to a pair of pions with low momentum P is

$$F=\mathrm{tr}\int\frac{d^3k}{(2\pi)^3}\phi^{-\dagger}(u^\dagger\chi_s u\phi^+ + \phi^+ v^\dagger\chi_s v), \tag{39}$$

where, for instance, we get for the scalar coupling $u^\dagger\chi_s u$ to the quark line

$$u_{s_1}(k)^\dagger\chi_s(k)u_{s_2}(k)=\frac{\delta_{s_1s_2}}{2\sqrt{2}}[(1-a)C\hat{k}\cdot\Delta(\hat{k}Sk\phi_s) -(1-3a)S\Delta(Ck\phi_s)] \tag{40}$$

except for the $-i$ factor which goes with any potential insertion according to the Feynman rules. We will discard it in this section. Integrating by parts, Eq. (39) can be simplified with the help of the mass gap equation and we get

$$F=\int\frac{d^3}{(2\pi)^3}\frac{k\phi_s}{\sqrt{2}}\left[-kS+\dot{\varphi}\frac{d}{dk}+aSC\Delta\right](\phi^{-\dagger}\phi^+) =\frac{0.011K_0^2-0.052M^2(P)}{f_\pi^2M(P)}K_0^{1/2}. \tag{41}$$

This coupling is very sensitive to the pion decay constant f_π and to the energy $M(P)$ of the pion.

We now consider the opposite limit of large pion momentum P. In this case the negative energy component of the pion is quite small. We expect that the dominant diagrams are the ones of the first line of Eq. (35), which include only the positive energy ϕ^+. This is present in either the coupling of a pion to the quark line, or the coupling of a π to an antiquark line,

$$F(P)=\int\frac{d^3k}{(2\pi)^3}\phi_s(k_1,0)(-\Delta_k')[\phi_p(k',P)\phi_p(k,-P)t_q + \phi_p(k,P)\phi_p(k',-P)t_{\bar{q}}]\Big|_{k'=k}, \tag{42}$$

where t_q and $t_{\bar{q}}$ are, respectively, the traces in Dirac indices

$$t_q=\mathrm{tr}\left\{\frac{-i\sigma_2}{\sqrt{2}}\vec{\sigma}\cdot\vec{k}_1u^\dagger(k_1)\Omega_l u(k_1')\frac{i\sigma_2}{\sqrt{2}}v^\dagger(k_2')\Omega_l u(k_2)\frac{i\sigma_2}{\sqrt{2}}\right\}$$
$$=\mathrm{tr}\left\{\frac{\vec{\sigma}\cdot\vec{k}_1}{\sqrt{2}}\frac{(1+\beta)}{2}\frac{(1+\vec{\alpha}\cdot\hat{k}_1)}{\sqrt{2}} \times\Omega_l\frac{(1+\vec{\alpha}\cdot\hat{k}_1')}{\sqrt{2}}\frac{1}{\sqrt{2}}\frac{(1+\beta)}{2}\gamma_5\frac{(1-\vec{\alpha}\cdot\hat{k}_2')}{\sqrt{2}} \times\Omega_l\frac{(1+\vec{\alpha}\cdot\hat{k}_2)}{\sqrt{2}}\frac{1}{\sqrt{2}}\right\} \tag{43}$$

and $t_{\bar{q}}$, of the second diagram, with the coupling of the pion to the antiquark yields the same result. The total coupling is a functional of the scalar and pseudoscalar wave functions, which are described in Eqs. (26), (35) by Gaussians. We now apply the Laplacian to the functions of k'. The dominant term of the expansion in $2/P$ comes from the derivatives of ϕ_P. A derivative of $\phi_P(k',P)$ will be proportional to $P/2$ when the Gaussian integral is performed, while a derivative of t_q or $t_{\bar{q}}$ which are functions of respectively $\hat{k}_1'$ or $\hat{k}_2'$ is proportional to $1/P$ and will not produce a dominant term. The traces then simplify to

$$t_q=t_{\bar{q}}=a\frac{k_1}{\sqrt{2}}[1-(\hat{k}_1\cdot\hat{k}_2)^2]. \tag{44}$$

We now apply the Laplacian to ϕ_P, and expand the $\hat{k}_1\cdot\hat{k}_2$ in a series of $1/P$. It is convenient to define $\alpha_T^2=2\alpha_s^2+\alpha_p^2$, and we get finally find for the momentum⊗spin contribution,

$$F(P)=\left[a\frac{-64\pi^{3/4}\alpha_s^{1/2}\alpha_p^2}{3^{1/2}(\alpha_p^2+\alpha_T^2)^2\alpha_T^3}\frac{P}{2}+o\left(\frac{2}{P}\right)\right]e^{-(p/2)^2/\alpha_T^2}, \tag{45}$$

where the dominant term is the a term which is of the order of 0.43 $K_0^{-1/2}$ for P of the order of $2K_0$.

The color factor for f_0 and π color singlets is $1/\sqrt{3}$. The flavor factor for the coupling of a scalar isosinglet $(u\bar{u}+d\bar{d})/\sqrt{2}$ to a pair of pseudoscalar isovectors, say $u\bar{d}$, and

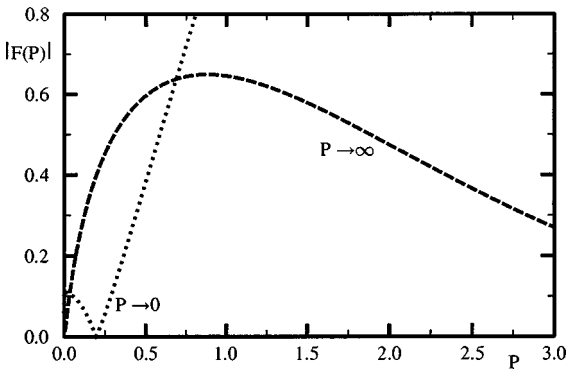

FIG. 7. We show $F(P)$, in the dimensionless units of $K_0=1$. The dotted and dashed lines correspond, respectively, to low P and high P limits.

$-d\bar{u}$, with a flavor independent quark-antiquark annihilation is $-1/\sqrt{2}$. The total coupling is then $-F(P)/\sqrt{6}$.

The function $F(P)$ is very cumbersome to derive in the case of intermediate momenta. For momenta of the order of K_0, see Fig. 7, matching the high and low P limits with an interpolating function is a possible approximation.

F. The $f_0(980)\rightarrow\pi\pi$ decay

The decay width of a f_0 in a pair of π can be calculated from the the Breit-Wigner pole in the meson propagator. We call the bare meson the one obtained from the ladder diagrams, see Eqs. (8), (C1), and (C13). The bare mass M_0 is real and is a solution of the Bethe-Salpeter equation. When coupled channels of mesons are included, the bare meson is dressed. The dressed pole is composed by the bare mass M_0 plus the coupled channel contribution which includes a real mass shift, and an imaginary term in the case where the mass is above the coupled thresholds. The mass is then

$$M = M_0 + \Delta M\ , \quad \Delta M = -i\Sigma$$

$\Sigma_{f_0} =$ 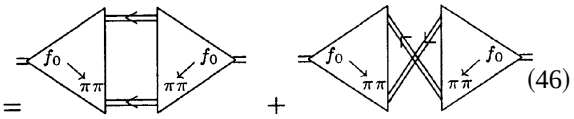 (46)

where we only included a loop of bare π, which is the simplest contribution to the scalar self-energy. The integral in the loop energy provides an extra $2\pi i$ factor, which implies that in general ΔM includes a real component, and we find that

$$\Delta M = 6\int \frac{d^3q}{(2\pi)^3}\frac{[F(q)^*/\sqrt{6}][F(q)/\sqrt{6}]}{M_{f_0}-2\sqrt{q^2+M_\pi^2}+i\epsilon}, \qquad (47)$$

where the factor of 6 includes the three different flavors of the isovector π, and the factor 2 from the direct and exchange diagram of the self-energy in Eq. (46). In this section we usually represent the width of a resonance by a Γ, which should not to be confused with the same symbol which is used in other sections for the vector or axial vertices. The width Γ is a simple function of the imaginary component of ΔM,

$$\mathrm{Im}(\Delta M) = -i\frac{\Gamma}{2}, \quad \Gamma = \frac{1}{4\pi}PM_{f_0}|F(P)^2|, \qquad (48)$$

where $P=\frac{1}{2}\sqrt{M_{f_0}^2-4M_\pi^2}$ is the momentum of the emitted π. Let us consider the case of a scalar mass M_{f_0} of the order of 1 GeV, where P is larger than the scale of the interaction by a factor of 1.4. In this case, it is sensible to use the limit of large momentum P for $F(P)$, see Eq. (45). We finally find a partial decay width of just 40 MeV for $F_0\rightarrow\pi\pi$ which lies within the experimental limits. We expect that a complete calculation without the large P approximation would not deviate from this by more than a factor of 2.

This result is also compatible with the narrow resonances $f_0(1500)$ and $a_0(980)$ which are possible ground states. Concerning $K_0^*(1430)$, which is wider and has decay products with a larger momentum P, the function $\Gamma(P)$ of Eq. (48) has the correct qualitative behavior of being proportional to P^3 for intermediate momenta. However in this model the exponential decrease is too strong, and the model needs some improvement in order to reproduce the correct $K_0^*(1430)$.

III. GOING BEYOND BCS WITH FINITE COUPLED CHANNEL EFFECTS

A. The mass gap equation and the self-energy

We find in Appendix D that the minimal extension of the mass gap equation beyond BCS is achieved with a new tadpole term in the self-energy

$\Sigma =$ 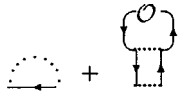 ,

$\mathcal{O}(\vec{k},w) =$ 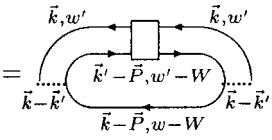 , (49)

D

where the subdiagram $\mathcal{O}$ is defined as an intermediate step. This amounts to extending the mass gap equation for the self-energy of the quarks with simple one meson exchange. Using the Weyl fermions, and expanding the ladder in meson poles, we find that the self-energy of the quark (antiquark) has a diagonal component Σ_d which contributes to the dynamical mass of the quark (antiquark)

$\Sigma_d =$ 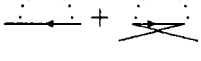 , (50)

and the energy of 1 quark is identical to the BCS energy of Eq. (19) except for the expected changes of the chiral angle φ. In Eq. (50) we only included the nonvanishing diagrams which remain from an expansion in powers of $1/U$. The free

Green functions are proportional to U^{-1}. The interactions without a pair creation or annihilation are proportional to the infinite infrared constant U, while the remaining interactions are finite. It turns out that the new coupled channel diagrams vanish. This happens because in the limit of an infinite $-U$ the box diagrams in Eq. (49) which contribute to the quark energy vanish. This is the case, for instance, of diagrams (a) and (b),

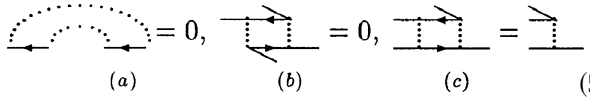

(51)

We find that the quark energy $E=E_0-\Sigma_d$ remains the BCS energy of Eqs. (16)–(19),

$$E(k)=u^\dagger(k)\vec{\alpha}\cdot\vec{k}u(k)-\frac{1}{2}\left\{u^\dagger(k)\int\frac{d^3k'}{(2\pi)^3}V(k-k')\times\Omega_l[\Lambda^+(k')-\Lambda^-(k')]\Omega_l u(k)\right\}. \quad (52)$$

However, the last diagram of Eq. (51), which contributes to the mass gap equation is finite.

The mass gap equation is obtained when we impose that the anti-diagonal components Σ_a of the self-energy must cancel. As in Eq. (16) this component is obtained with the projection of the spinors $u^\dagger$ and v. This produces a function Σ_a with the quantum numbers of a scalar, see Eqs. (20) and (22). In order to use the results of the preceding section, it is convenient to fold Σ_a with a generic scalar wave function $\phi^+_{f_0}$. Then the resulting product must vanish for any $\phi^+_{f_0}$. In fact this ensures vacuum stability since this prevents the vacuum to decay in scalar modes. The diagrams that contribute to the antidiagonal component of the self-energy in the mass gap equation are now

$tr\left\{\phi^+_{f_0}(k)^\dagger\Sigma_a\right\}=$

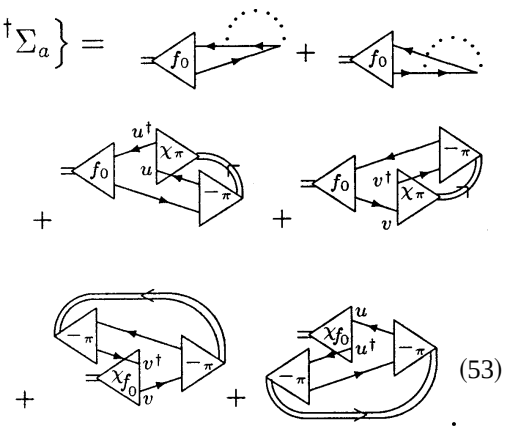

(53)

In Eq. (53) we only show the diagrams which are nonvanishing in orders of $1/U$, and in fact they all are finite, of order U^0. The first pair of diagrams are BCS diagrams. It turns out that the new diagrams are the same diagrams which contribute to the $f_0\to\pi\otimes\pi$ coupling, except for the negative energy wave function of the π and for the integral in the π momentum P. The negative energy wave function ϕ^- always vanishes for high momentum P, and in the case of low momentum P it is relevant only for the pseudoscalar family of the π. We suppose that the large number of excited states is not sufficient to compensate the smallness of ϕ^-, and we will not consider this ultraviolet problem. Thus we will only include the coupled channel contribution of the π family. In the case of low momentum, the π family has a extremely large ϕ^-, however, the coupling to a quark $u^\dagger\chi u$ is derivative and vanishes. This prompts us to neglect the last line of Eq. (53). Finally we can remove, with a functional derivative, the generic scalar wave function $\phi^+_{f_0}$. The result after integrating in all the loop energies can be represented,

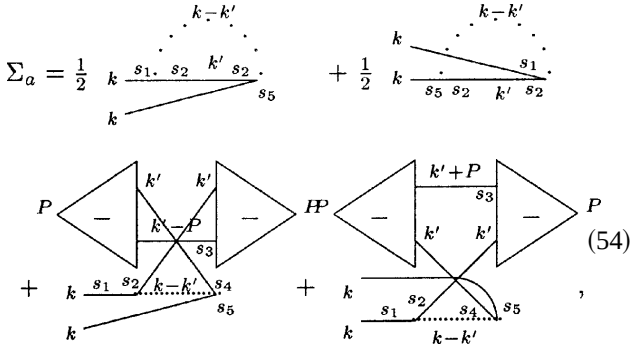

(54)

where the lines only represent the spinors u, v, $u^\dagger$, or $v^\dagger$, the integrals and the traces and no longer include the quark or antiquark propagators. The mass gap equation $0=S_0^{-1}{}_a-\Sigma_a$ is now

$$0=+u^\dagger_{s_1}(k)\vec{\alpha}\cdot\vec{k}v_{s_5}(k)-\left\{u^\dagger_{s_1}(k)\int\frac{d^3k'}{(2\pi)^3}V(k-k')\Omega_l+\left[u_{s_2}(k')\left(\frac{\delta_{s_2s_4}}{2}-\int\frac{d^3P}{(2\pi)^3}\phi^-_{s_2s_3}(P,k'-P/2)\times\phi^-_{s_3s_4}{}^\dagger(P,k'-P/2)\right)u^\dagger_{s_4}(k')-v_{s_2}(k')\times\left(\frac{\delta_{s_2s_4}}{2}-\int\frac{d^3P}{(2\pi)^3}\phi^-_{s_2s_3}{}^\dagger(P,k'-P/2)\phi^-_{s_3s_4}\times(P,k'-P/2)\right)v^\dagger_{s_4}(k')\right]\Omega_l v_{s_5}(k)\right\}, \quad (55)$$

where the sum over repeated spin indexes s_i is assumed.

B. Model independent effects of the coupled channels

The dominant effect of coupled channels in Eq. (55) is to multiply the potential term in the mass gap equation (16) by a factor of

$$1-2\int\frac{d^3P}{(2\pi)^3}\phi^-_p\phi^{-\dagger}_p. \quad (56)$$

This clearly decreases the term which is the source for the spontaneous breaking of chiral symmetry. Thus the coupled channel effect is to restore partially the chiral symmetry. This effect is independent of the quark-quark interaction.

The signs of the new terms in the mass gap equation deserve a special attention since they determine whether the coupled channel effect will increase or decrease the chiral condensation. Because the coupled channel terms introduce in the mass gap equation a new fermion loop it is natural for Dirac fermions that the coupled channel terms should be affected with a minus sign.

When the Dirac fermions are translated into Weyl fermions the quarks divide into the species of quarks and antiquarks which have independent field operators and propagators, and the minus signs are transfered from the propagator and the loops into the antiquark vertex and the exchange diagrams, and loops with quarks (antiquarks only). In this case we check with Weyl fermions that the minus sign persists and is due to the quark (antiquark) exchange. Only retardation, which was not included here, might perhaps oppose to this negative sign.

This sign can also be understood from the perspective of the Mexican hat potential $-\lambda\sigma^2+\mu\sigma^4$ of effective meson models. In this case the quadratic term spontaneously creates a scalar condensate, while the quartic term opposes to the condensation and the actual condensate corresponds to the minimum of the energy density where the two terms are balanced. In the present paper there are three terms, a kinetic term which opposes to the condensate (and has no correspondence in the effective meson models), a BCS term which spontaneously breaks chiral symmetry (it is equivalent to the quadratic term of effective meson potentials), and a beyond BCS term which is equivalent to the quartic term in effective meson potentials. This correspondence, which is supported by the mean field theory where $\langle\bar{\psi}\psi\rangle\simeq\sigma$, confirms the negative sign of the coupled channel term. Thus we may assume quite generally that coupled channels oppose to the breaking of chiral symmetry.

An interesting feedback from chiral symmetry to the narrow width the ground state occurs. Chiral symmetry breaking can be understood variationally, the solution $\varphi(k)$ of the mass gap equation also minimizes the energy density $\mathcal{E}$ of the vacuum. $\mathcal{E}$ is the sum of three terms, the free one, the BCS one and the beyond BCS one. Only the BCS term is negative and drives $\varphi(k)$ away from the trivial vanishing solution. The actual solution $\varphi(k)$ minimizes the free term *and minimizes the beyond* BCS *term* and at the same token produces the most negative BCS term. In Eq. (53), we saw that the beyond BCS diagrams in the mass gap equation are similar to the diagrams of coupling of a scalar to a pair of pseudoscalars (with low to moderate momentum). Thus we conclude that this coupling is naturally suppressed and that this suppression is selective in the sense that it should not occur in other hadronic couplings. This has an amplified effect in the scalar width which is a function of the square of this coupling.

C. Solution of the mass gap equation

We will now focus on the dominant terms among the coupled channel contributions. We obtain the momentum⊗spin coupled channel contribution

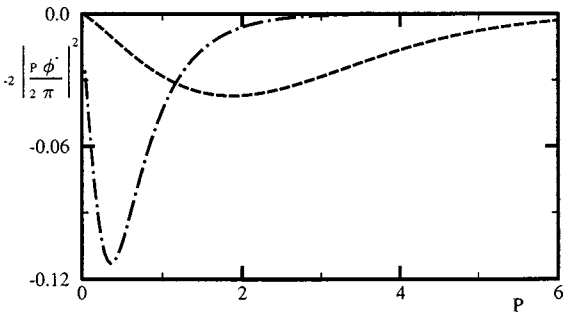

FIG. 8. We show the integrand of $\xi(0)$, in the dimensionless units of $K_0=1$. The dotted and dashed lines correspond, respectively, to the cases where ϕ is obtained in the low P limit and in the high P limit.

$$\xi=\int dPdw\,\frac{-2P^2\phi^-(k+P/2)\phi^-(k+P/2)^\dagger}{(2\pi)^2}. \quad (57)$$

From Eqs. (27), (35) we get for the integrand of Eq. (57),

$$P\to 0,\quad -0.14\frac{P^2}{M(P)}\left[S(k_1)-M(P)\frac{f_1(k_1)}{k_1}\right]^2,$$

$$P\to\infty,\quad -1.9\frac{a^2P^{5/4}}{(1-a)^{11/4}}e^{-k_1^2/\alpha_p^2}, \quad (58)$$

where the spin factor $(i\sigma_2/\sqrt{2})(-i\sigma_2/\sqrt{2})=\frac{1}{2}$ is included. The integral that leads to ξ is now evaluated with an interpolation between the two limits of Eq. (58), see Fig. 8. Because this interpolation is arbitrary, we have to include in the result a theoretical error.

We obtain the momentum⊗spin coupled channel contribution

$$\xi(k)=-(0.4\pm 0.1)S \quad (59)$$

which turns out to have a shape very close to the function $S=\sin(\varphi)$ which was evaluated at the BCS level. We estimate that the coupling to the quasi-Goldstone bosons, including the momentum, spin, color, and flavor contributions yields

$$\xi(k)\simeq-(0.4\pm 0.1)S\frac{1}{3}\left(N_f-\frac{1}{N_f}\right)$$
$$\simeq-(0.3\pm 0.2)S,\quad N_f=2\to 3. \quad (60)$$

N_f is the number of almost massless quark flavors which empirically is between 2 and 3.

The mass gap equation can be solved for a coupled channels contribution equal to ξ, when $\xi\geqslant -1$,

$$0=u^{\dagger}\left[\vec{\alpha}\cdot\vec{k}-\frac{1}{2}\Omega_l\int V(\Lambda^{+}-\Lambda^{-})(1+\xi)\Omega_l\right]v$$
$$=\left\{kS-[1-a(2C^2+1)]\left[\frac{\Delta\varphi}{2}(1+\xi)+\dot{\xi}\dot{\varphi}\right]\right.$$
$$\left.-SC\left[\frac{1}{k^2}+a\left(\dot{\varphi}^2-\frac{1}{k^2}\right)\right](1+\xi)+aSC\Delta\xi\right\}\vec{\sigma}\cdot\hat{k}i\sigma_2. \tag{61}$$

The solution φ for $\xi=-0.3S_{\mathrm{BCS}}$ is shown in Fig. 5. In this case and for the same parameter K_0, quark condensate $\langle\bar{\psi}\psi\rangle$ is decreased by a factor of $(1-0.12)^3$.

IV. RESULTS AND CONCLUSION

We developed a general formalism to include both the effects of chiral symmetry breaking and strong hadron-hadron interactions in quark models. This is encouraging since both effects are firmly established in phenomenology. We find new general effects in the scalar meson width, in the breaking of chiral symmetry and in the mass shifts of the hadron spectrum. Quantitative results are computed within a model which belongs to a class of Nambu and Jona-Lasinio absolutely confining instantaneous interactions, in the case where the coupled pair of mesons are accounted as bare mesons.

We find in this model that the mass and width of the light $q\bar{q}$ scalar f_0 meson are close [11] to the experimental mass and width of the $f_0(980)$, and not to the $f_0(400-1200)$ or the $f_0(1370)$. This apparently indicates a possible solution to the scalar meson puzzle without meson molecules, glueballs, or strongly nonlinear coupled channel effects. In this case the attraction which is visible in $\pi\pi$ phase shifts and in the intermediate range *NN* interactions would need other interpretations [30] than the very wide σ meson.

Compared with χSB at the BCS level, a new parameter has been identified, which leads to the percentage of coupled channel effects in the mass gap equation. We find that coupled channels suppresses the breaking of chiral symmetry. This results are model independent. With our model we get a suppression of the quark condensate by $5\rightarrow 55\%$ when the coupled channel effects are included.

We find a new interesting feedback mechanism from chiral symmetry to coupled channels and explain it variationally. The chiral symmetry restorating contribution to the mass gap equation from coupled channels is closely related to the coupling of a scalar to a pair of pseudoscalars. The feedback enforces that the width of a ground state scalar decaying to a pseudoscalar pair (with low or moderate momentum) is reduced when compared to the width of any other resonance. This effect is model independent and contributes to understand the scalar meson puzzle.

Concerning real mass shifts we estimate that they are canceled due to the new terms which are introduced by the Ward identities. This might improve previous [4,12] coupled channel calculations where this cancellation was not explicitly included. A systematic shift of the hadron spectrum is not expected. In this sense we agree with the results of Geiger and Isgur [31]. Nevertheless mass splittings between states with different quantum numbers are still expected from the bound state equation. Different theoretical problems that could be reviewed with these new techniques are the contribution of the coupled channels to the hadron spectra, for instance, to the interesting η' mass or to the nucleon mass. We conclude that in general the results of this paper, without ruling out other perspectives, explain why the naive quark model is so successful.

ACKNOWLEDGMENTS

I am very grateful to Emilio Ribeiro for long discussions and suggestions since 1989 on the pion mass problem in relation with the coupled channels, on the BCS mechanism, and on Ward identities. I also acknowledge George Rupp, Jean-Marc Richard, Jack Paton, Robin Stinchcombe, Nils Tornqvist, Vitor Vieira, Pedro Sacramento, and Adam Szczepaniak for comments or suggestions. I thank Sid Coon for a careful reading of the manuscript.

APPENDIX A: CONFINEMENT WITH INFRARED FINITE COUPLED CHANNELS

At the BCS level, the bound states are obtained with the ladder approximation which is equivalent to the Salpeter equation, and to the Schrödinger equation (see Appendix C). In this case the infinite infrared divergent constant U of the interaction (4), (5) is extremely convenient [23] to remove the colored states, which have masses proportional to U. Let us consider the dominant terms in orders of U of the energy of a system of n quarks and antiquarks. The one-body energy includes the self-energy (19) which is calculated with the Schwinger-Dyson equation

$$\sum_i E_i+\sum_{i<j}V_{ij}\simeq\frac{3}{4}\left(\frac{U}{2}\sum_i\frac{\vec{\lambda}_i}{2}\cdot\frac{\vec{\lambda}_i}{2}+U\sum_{i<j}\frac{\vec{\lambda}_i}{2}\cdot\frac{\vec{\lambda}_j}{2}\right)$$
$$\simeq\frac{3}{32}U\vec{\Lambda}\cdot\vec{\Lambda}, \tag{A1}$$

where $\vec{\Lambda}$ is the Gell-Mann matrix of the total color of the system. The energy (A1) vanishes for color singlets only, while colored states have an infinite energy and in this sense are confined.

To include coupled channels in the energy of a color singlet, for instance, in a meson, we consider the complete series of diagrams that contribute to the irreducible $q\bar{q}$ interaction. One has to include all the possible number of quark loops and all the possible insertions of the microscopic quark-quark interaction. Then this series can be resumed in order to factorize the bare meson $(q\bar{q})$ and hadron (qqq) ladders. According to Appendix C, the ladder needs integrals $\int(dw/2\pi)$ in all the external relative energies in order to have a hadron pole. To ensure, in a particular diagram, that the meson poles are present, it is convenient to decompose the ladder as

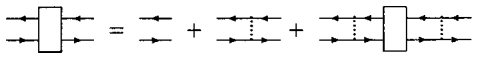

(A2)

where in the right-hand side the ladder is integrated and contains the meson pole, and the first pair of diagrams contributes to the overlap interactions of hadrons. In order to simplify the calculations it is convenient to truncate eventually the series of diagrams. The pertubative parameter is then the number of considered ladders. This is both straightforward and also close to the hadronic phenomenology.

We now show how the interactions of color singlet ladders can be finite, when they are built from the infrared divergent quark-quark microscopic interaction (5), and the quark propagators are divergent as well. When a hadron is emitted or absorbed we have quark-antiquark annihilation overlaps, for instance, in a three-meson vertex,

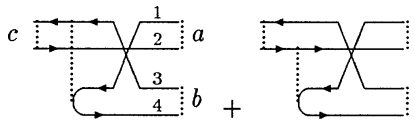

(A3)

We first integrate the relative energies in the first diagrams of Eq. (A3),

$$\int \frac{dwdw'}{(2\pi)^2}\frac{i}{w-E_1+i\epsilon}iV_{\overline{14},3}\frac{i}{-w'-E_4'+i\epsilon}$$
$$=\frac{i}{w'-E_3'+i\epsilon}\frac{i}{w-E_3+i\epsilon}\frac{i}{-w-E_2+i\epsilon}$$
$$=-iV_{\overline{14},3}G_{0_a}G_{0_b}G_{0_c}, \tag{A4}$$

where the G_{0_n} are in fact part of the respective BS amplitudes which are untruncated. The remaining factor $-iV_{\overline{14},3}$ is finite because the term proportional to U in the quark-antiquark annihilation vertex is $v_s^\dagger(k)\delta^3(k-k')u_{s'}(k')=0$.

When the number of hadrons are conserved, this is the case in elastic scattering, we have quark exchange overlaps, for instance, in a four-meson vertex

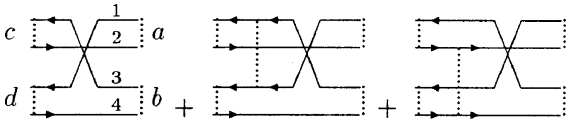

(A5)

The integrals in the relative energies are

$$\int \frac{dw}{2\pi}\frac{i}{w-E_1+i\epsilon}\frac{i}{-w-E_4+i\epsilon}\frac{i}{w-E_3+i\epsilon}\frac{i}{-w-E_2+i\epsilon}$$
$$=i(E_1+E_2+E_3+E_4)G_{0_a}G_{0_b}G_{0_c}G_{0_d},$$

$$\int \frac{dwdw'}{(2\pi)^2}\frac{i}{w-E_1+i\epsilon}(-iV_{13})$$
$$\times\frac{i}{w'-E_1'+i\epsilon}\frac{i}{-w'-E_4'+i\epsilon}$$
$$\times\frac{i}{w'-E_3'+i\epsilon}\frac{i}{w-E_3+i\epsilon}\frac{i}{-w-E_2+i\epsilon}$$
$$=-iV_{13}G_{0_a}G_{0_b}G_{0_c}G_{0_d}. \tag{A6}$$

The four G_{0_n}, will be absorbed by the Salpeter amplitudes and the remaining factors are

$$i(E_1+E_2+E_3+E_4-V_{13}-V_{24})P_{13}$$
$$=i(E_1+E_2+E_3+E_4+V_{14}+V_{23})P_{13}$$
$$=iP_{13}(E_1+E_2+V_{12}+E_3+E_4+V_{34})$$
$$=iP_{13}(0U+\cdots), \tag{A7}$$

where the infinite $-U$ terms cancel in the same way as in Eq. (A1) because the mesons 32 and 14 in the left and 12 and 34 in the right are color singlets. We find that all the terms proportional to U cancel when the complete set of diagrams which contribute to the interaction between color singlets is included.

In this framework the masses of bare hadrons and their interactions are finite and can be evaluated. Then we compute the masses and widths of dressed hadrons. These are the final freedom degrees which can be compared with the experimental spectrum of hadronic resonances.

APPENDIX B: THE LIGHT π AND WARD IDENTITIES

The solution to the pion mass problem is found using [22,32] the Ward identities (WI) in order to insure that the bound state equation for the pion—a Bethe-Salpeter equation with coupled channels—is consistent with the non linear mass gap equation. The WI were first derived for fermion-gauge field theories, and were initially based on the simple observation that for free fermions with propagator $\mathcal{S}_0(p)=i/(\not{p}-m_0)$ and a free vector vertex $\Gamma_0^\mu=\gamma^\mu$,

$$i(p_\mu-p'_\mu)\mathcal{S}(p)\Gamma^\mu(p,p')\mathcal{S}(p')=\mathcal{S}(p)-\mathcal{S}(p'). \tag{B1}$$

The difference in the right-hand side of the equation extends the identity to renormalized propagators and vertices. This identity is then crucial for the conservation of electric charge. The WI enforce that the self-energy of the MGE is obtained (without double counting) from the BS kernel by closing the fermion line where the vertex is inserted. Inversely, they also ensure that the BS kernel is obtained if one inserts the vertex in all possible propagators of the self-energy. For instance this mapping is trivial at the BCS level where the mass gap equation (6) is clearly equivalent to the bound state equation (7). Let us now consider a more general case, where the fermion self energy include a product of bare propagators

$S_{\alpha_i\beta_i}(k_i+P)$. The external momentum is P and k_i is a loop momentum. The propagators can be factorized and we get

$$\Sigma(P)=\cdots\prod_i S_{\alpha_i\beta_i}(k_i+P). \tag{B2}$$

Then the vertex Γ can be constructed if we insert a bare vertex in all possible bare propagators, and we get

$$\Gamma^\mu(P_1-P_2)=\cdots\sum_j \prod_{i1\leqslant j} S_{\alpha_{i1}\beta_{i1}}(k_{i1}+P_1)\gamma^\mu \times\prod_{i2\geqslant j} S_{\alpha_{i2}\beta_{i2}}(k_{i2}+P_2). \tag{B3}$$

Conversely the original self-energy can be recovered if we substitute the bare vertex by the difference of propagators

$$i(P_{1\mu}-P_{2\mu})\Gamma^\mu=\cdots\sum_j \prod_{i1<j} S_{\alpha_{i1}\beta_{i1}}(k_{i1}+P_1),$$

$$[S_{\alpha_j\beta_j}(k_j+P_1)-S_{\alpha_j\beta_j}(k_j+P_2)]\prod_{i2>j} S_{\alpha_{i2}\beta_{i2}}(k_{i2}+P_2) =[\Sigma(P_1)-\Sigma(P_2)], \tag{B4}$$

where the products which depend on both P_1 and P_2 cancel, and this removes the double counting.

There is also a WI identity for the free axial vector vertex $\Gamma_f^{\mu 5}=\gamma^\mu\gamma^5$ that involves the free pseudoscalar vertex $\Gamma_f^5=\gamma^5$,

$$-i(p_\mu-p'_\mu)\mathcal{S}(p)\Gamma^{\mu 5}(p,p')\mathcal{S}(p') +2\,\mathrm{im}\,\mathcal{S}(p)\Gamma^5(p,p')\mathcal{S}(p')=\mathcal{S}(p)\gamma^5+\gamma^5\mathcal{S}(p') \tag{B5}$$

which is valid in a renormalization program providing the interaction is chirally invariant. In this case an equation analogous with Eq. (B5) is made up of the axial and pseudoscalar vertices and the self-energy.

A key product of the axial WI is the proof [7,33] that a pseudoscalar Goldstone boson exists when current quark masses vanish and chiral symmetry breaking occurs. The full propagator is then renormalized and the self-energy Σ has a masslike term

$$\mathcal{S}^{-1}(p)=\mathcal{S}_0^{-1}(p)-\Sigma(p),\quad i\Sigma=A(p)-\not{p}B(p), \tag{B6}$$

$$\mathcal{S}^{-1}(p)=\mathcal{S}_0^{-1}(p)-\Sigma(p)=\frac{A(p)\not{p}-B(p)}{i}. \tag{B7}$$

If we substitute this propagator in the WI, we find the solution for the pseudoscalar vertex Γ^5 with a vanishing $p-p'$,

$$\Gamma^5(p=p')=\frac{B(p)}{m_0}\gamma^5 \tag{B8}$$

which diverges for a vanishing quark mass m_0 and shows that the pole of a massless pseudoscalar meson appears in the axial vector vertex, with a bound state truncated amplitude of

$$\chi(p-p'\simeq 0)=\frac{B\gamma_5}{f_\pi}, \tag{B9}$$

where f_π includes a norm. Incidentally, this identity also offers a proof of the Gell-Mann, Oakes, and Renner relation. If we expand the vertex Γ^5 in the neighborhood of the π pole,

$$\Gamma^5=\chi\frac{i}{(p-p')^2-M^2}\,\mathrm{tr}\{\chi\mathcal{S}(p)\Gamma_0^5\mathcal{S}(p')\}, \tag{B10}$$

where we included the integral in the trace. Substituting Γ_5 in Eq. (B8) and performing a trace with $\mathcal{S}\gamma_5\mathcal{S}$, we find for small masses

$$\mathrm{tr}\left\{\gamma_5\frac{B\mathcal{S}\gamma_5\mathcal{S}}{f_\pi}\right\}\frac{i}{-M^2}\,\mathrm{tr}\left\{\frac{B\mathcal{S}\gamma_5\mathcal{S}}{f_\pi}\gamma_5\right\} =\mathrm{tr}\left\{\gamma_5\frac{B\mathcal{S}\gamma_5\mathcal{S}}{m_0}\right\}\Rightarrow -m_0\,\mathrm{tr}\{\mathcal{S}\}=-2m_0\langle\bar{\psi}\psi\rangle=M^2f_\pi^2. \tag{B11}$$

In QCD it is necessary to include the axial anomaly, in the flavor singlet WI which corresponds to the η' channel. The flavor octet axial currents remain unchanged, in particular the π, K, η remain quasi-Goldstone bosons. We will now simply assume that the η' is heavier [2,7,17,34] than the usual N_f^2-1 Goldstone bosons, where N_f is the number of light quark flavors.

APPENDIX C: THE SALPETER EQUATIONS IN THE ENERGY-SPIN FORMALISM

When the interaction is instantaneous, a simplification occurs in the Bethe-Salpeter S matrix in the ladder approximation

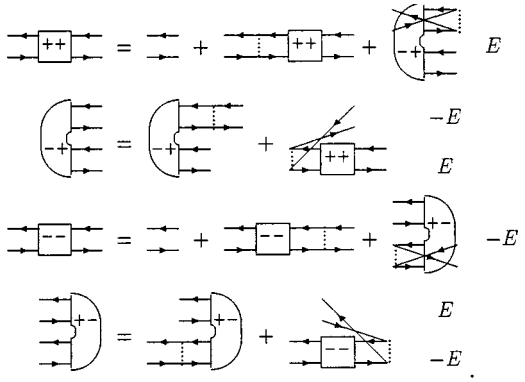

(C1)

The S matrix only has four independent submatrices, which have to be calculated iteratively. The other 12 submatrices are directly computed from the independent four ones. The

Salpeter equations are obtained when all the relative quark-antiquark energies of the system (C1) are integrated,

$$\int \frac{dw}{2\pi} \frac{i}{w+W/2-E_q+i\epsilon} \frac{i}{w+W/2-E_{\bar{q}}+i\epsilon} = \frac{i}{W-E_q-E_{\bar{q}}+i\epsilon}. \tag{C2}$$

The Salpeter equations can then be written in the compact form

$$S=G_0+G_0VS \Rightarrow (G_0^{-1}-V)S=1 \Rightarrow (W\sigma_3-H+i\epsilon)S=i, \tag{C3}$$

where σ_3 is the Pauli matrix,

$$S=\begin{bmatrix} S^{++} & S^{+-} \\ S^{-+} & S^{--} \end{bmatrix},$$

$$G_0=\begin{bmatrix} \dfrac{i}{W-E_q-E_{\bar{q}}+i\epsilon} & 0 \\ 0 & \dfrac{i}{-W-E_q-E_{\bar{q}}+i\epsilon} \end{bmatrix},$$

$$V=-i\begin{bmatrix} \int V_d & \int V_a \\ \int V_a & \int V_d \end{bmatrix},$$

$$H=\begin{bmatrix} E_q+E_{\bar{q}}+\int V_d & \int V_a \\ \int V_a & E_q+E_{\bar{q}}+\int V_d \end{bmatrix} \tag{C4}$$

and it turns out that H is a Hermitian and positive operator. The Salpeter wave-functions are the solutions of the homogeneous equations,

$$(M\sigma_3-H)\phi=0, \phi=\begin{pmatrix} \phi^+ \\ \phi^- \end{pmatrix}, \tag{C5}$$

which is an eigenvalue equation, similar to the Schrödinger equation, except for the σ_3. This formalism is known as the energy-spin formalism, where ϕ^+ is called the positive energy wave-function and ϕ^- is called the negative energy wave function. The Salpeter equation (C5) is equivalent to the variational equation

$$\delta\left(\frac{\langle\phi|H|\phi\rangle}{\langle\phi|\sigma_3|\phi\rangle}\right)=0, \tag{C6}$$

which suggests that a normalizing condition of the wave functions might be

$$\langle\phi|\sigma_3|\phi\rangle=|\phi^+|^2-|\phi^-|^2=1. \tag{C7}$$

Let us study the class of solutions ϕ_u where this norm is possible, i.e., $|\phi_u^+|>|\phi_u^-|$. Once the single quark energies E and the two-quark diagonal V_d and antidiagonal V_a potentials are defined, the solutions can be obtained numerically, either iteratively or variationally, and one finds a whole spectrum of solutions with energy $M>0$. When M increases, we find that $|\phi_u^-|$ is proportional to M^{-1}, and in the limit of large mass we exactly recover Schrödinger equation. However, another class of solutions ϕ_d is unavoidable, with a one to one correspondence with the ϕ_u, and where $|\phi_d^-|>|\phi_d^+|$,

$$\phi_d^+=\phi_u^-, \quad \phi_d^-=\phi_u^+, \quad M_d=-M_u,$$
$$\langle\phi_u|\sigma_3|\phi_u\rangle=1, \quad \langle\phi_d|\sigma_3|\phi_d\rangle=-1, \tag{C8}$$

thus the spectrum is unbound. Exactly half of the solutions have a negative mass and a negative norm. When we include the infinitesimal $i\epsilon$ in Eq. (C5), we find that the larger component of ϕ dominates and the eigenvalues are now

$$M_u \to M_u - i\epsilon,$$
$$M_d \to M_d + i\epsilon = -(M_u - i\epsilon). \tag{C9}$$

The operators H and σ_3 are both Hermitian, thus the set of solutions $|\phi\rangle$ constitute a basis of the Hilbert space, orthogonal in the sense that $\langle\phi|\sigma_3|\phi'\rangle=0$, and the identity element is

$$1=\sum \frac{\sigma_3|\phi\rangle\langle\phi|}{\langle\phi|\sigma_3|\phi\rangle}=\sum_u \sigma_3|\phi_u\rangle\langle\phi_u|-\sum_d \sigma_3|\phi_d\rangle\langle\phi_d|. \tag{C10}$$

Inserting this partition in the S matrix equation (C3), we find

$$i=(W\sigma_3-H)S=\sum \frac{\sigma_3|\phi\rangle\langle\phi|}{\langle\phi|\sigma_3|\phi\rangle}(W\sigma_3-H + i\epsilon)\sigma_3\sum \frac{\sigma_3|\phi\langle\phi|}{\langle\phi|\sigma_3|\phi\rangle}\sigma_3 S$$
$$=\sum \sigma_3|\phi\frac{W-M+i\epsilon\langle\phi|\sigma_3|\phi\rangle}{\langle\phi|\sigma_3|\phi\rangle}\langle\phi|\sigma_3 S,$$
$$\sigma_3 S=\sum \sigma_3|\phi\rangle\frac{i\langle\phi|\sigma_3|\phi\rangle}{W-M+i\epsilon\langle\phi|\sigma_3|\phi\rangle}\langle\phi|,$$
$$S=\sum_u |\phi_u\rangle\frac{i}{W-M_u+i\epsilon}\langle\phi_u|-\sum_d |\phi_d\rangle\frac{i}{W-M_d-i\epsilon}\langle\phi_d| \tag{C11}$$

and the states with negative energy and negative norm can be reinterpreted as bound states with positive mass moving forward in time, where the variable $W=P_0$ in the propagator turns out to be negative,

$$S=\sum_u |\phi_u\rangle\frac{i}{W-M_u+i\epsilon}\langle\phi_u|+\sigma_1|\phi_u\rangle \times\frac{i}{-W-M_u+i\epsilon}\langle\phi_u|\sigma_1 \tag{C12}$$

and it suffices to work with the ϕ_u. Diagrammatically we get, for instance,

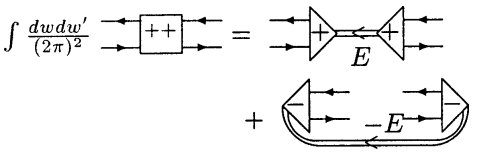

(C13)

where w and w' are the external energies. The quark antiquark BS amplitude is represented by the triangle $\Rightarrow$ and the boson propagator of the meson is represented by the double line $=$. It is consistent to substitute the $_d$ wave functions and masses in terms of the components ϕ_u^+, ϕ_u^- and the masses M_u. In the paper this reinterpretation will be assumed and we will skip the subindex $_u$. The practical result is that we can use the amplitude ϕ^+ when the bra(ket) precedes(succeeds) the meson propagator, and we use the amplitude ϕ^- for the opposite case.

APPENDIX D: THE BETHE-SALPETER EQUATION WITH COUPLED CHANNELS

We now go beyond BCS including the mesonic coupled channels both in the MGE and in the bound state equations. It is convenient to return to the Dirac formalism in order to reduce the number of diagrams when we apply the WI. We will extend the BS for the $q\bar{q}$ bound state of the quarks with the minimal meson loop of coupled channels

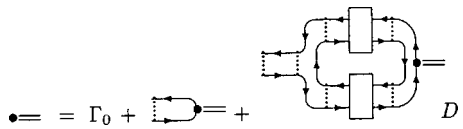

(D1)

where we follow the approximation of including only three-legged effective meson vertices in the meson interaction. We will show that this is imposed by the box at the left of the ''beyond BCS'' diagram in Eq. (D1). Upon iteration the equation

$$\Gamma = \Gamma_0 + VG_0\Gamma + VG_0VM\Gamma \tag{D2}$$

can be resummed. If we factorize the S matrix at the ladder level $S_0 = (1 - G_0V)^{-1}G_0$, see Eq. (C3), the ladder will appear in the middle of the coupled channel terms,

$$G_0\Gamma = S_0\Gamma_0 + G_0VS_0VM\Gamma,$$

$$\Gamma \simeq VS_0\Gamma_0 + VS_0VM\Gamma. \tag{D3}$$

When the ladders S_0, including the two ones of the meson loop in M, are expanded in meson poles and wave functions according to Eq. (C13), we recover the meson-meson pair coupling of Eq. (37). The resulting pole of the vertex Γ is the mass of the dressed meson $M_0 + \Delta M$. This procedure is equivalent to the resonating group method equations [29] for coupled channels of one meson with a pair of noninteracting mesons.

We now use the WI prescription of removing the vertex and closing the respective fermion line to arrive at the mass gap equation (49). To recover the full vertex equation we must insert the vertex in all possible propagators of Eq. (49). We then arrive at a WI consistent Bethe-Salpeter equation for the vertex and for the bound state,

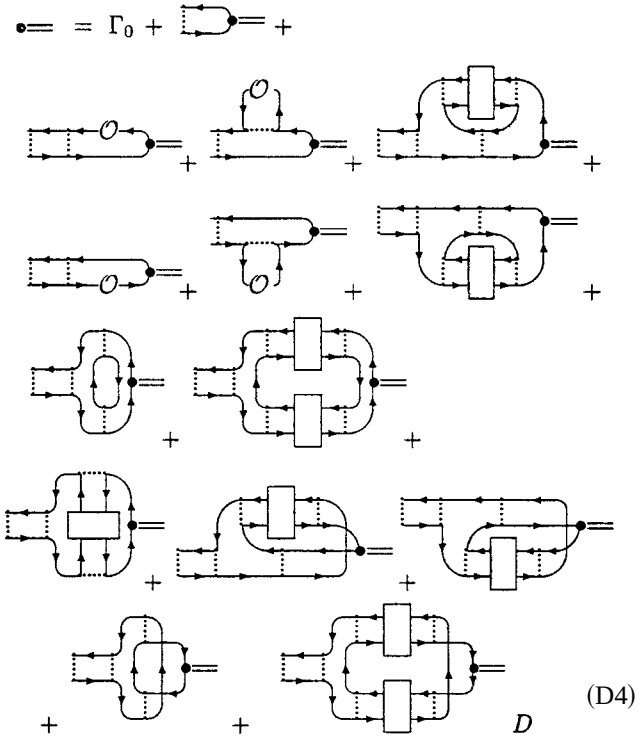

(D4)

where the diagrams are shown in separate lines according to their properties. Line 1 corresponds to the BS equation at the BCS level. Without the other lines it would reproduce the ladder Bethe-Salpeter equation for the vertex. The lines 2, 3, and 5 were separated because they contain all the terms proportional to the infrared divergent U, but they cancel in each line and all lines are finite. The remaining lines 4 and 6 contain the terms that one would expect in coupled channel equations where a pair of mesons is created and then annihilated (except for the first diagrams of line 4 and line 6 which vanish). With them we calculate for instance the partial decay width of a resonance into a channel of two mesons. The last lines 5 and 6 are only relevant for flavor singlets because the quark pair in the incoming meson is annihilated, thus for flavor vectors they are null.

The cancellation of the infrared divergences becomes clear in the Goldstone-Weyl formalism. Let us consider for instance the diagrams of line 2 in Eq. (D4),

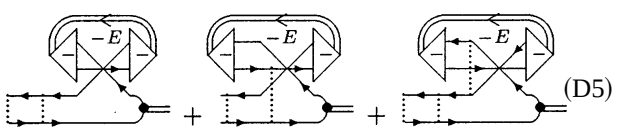

(D5)

These three diagrams are infrared divergent but their sum is finite, in an analogous way to Eq. (A5).

It is important to remark that in the previous calculations in the literature, the extrapolation from the ladder level to the coupled channel level would only include the diagrams of lines 4 and 6. We now find the previous choice arbitrary since the diagrams of lines 2, 3, and 5 were not considered. The role of these diagrams is to cancel any real mass shift of the π due to the usual coupled channel diagrams of lines 4 and 6, in order that the π remains a Goldstone boson in the chiral limit. This is ensured by the WI, see Eq. (B8). Concerning widths, since the new diagrams are real, the results of the previous calculations in the literature are correct. However we find no systematic real mass shift in the meson spectrum due to coupled channels. This contradicts most of the real mass shifts of hundreds of MeV which are common in the literature. Only splittings between different levels, due to neighboring cuts, may be affected by coupled channels.

[1] Particle Data Group, R. M. Barnett *et al.*, Phys. Rev. D **54**, 1 (1996).

[2] A. Szczepaniak, E. Swanson, C.-R. Ji, and S. Cotanch, Phys. Rev. Lett. **76**, 2011 (1996).

[3] J. Weinstein and N. Isgur, Phys. Rev. Lett. **48**, 659 (1982); Phys. Rev. D **27**, 588 (1983).

[4] E. Van Beveren, T. Rijken, K. Metzger, C. Dullemond, G. Rupp, and J. Ribeiro, Z. Phys. C **30**, 615 (1986).

[5] N. Törnqvist and M. Roos, Phys. Rev. Lett. **76**, 1575 (1996); N. Tornqvist, Z. Phys. C **68**, 647 (1995).

[6] J. Bardeen, L. N. Cooper, and J. R. Schrieffer, Phys. Rev. **108**, 1175 (1957); L. V. Keldysh, and A. N. Kozlov, Sov. Phys. JETP **27**, 521 (1968).

[7] Y. Nambu and G. Jona-Lasinio, Phys. Rev. **122**, 345 (1961); **124**, 246 (1961).

[8] F. T. Hawes and A. G. Williams, Phys. Lett. B **268**, 271 (1991); A. Bashir and M. R. Pennington, Phys. Rev. D **50**, 7679 (1994); H. J. Munczek, *ibid.* **52**, 4736 (1995); A. Bender, C. D. Roberts, and L. V. Smekal, Phys. Lett. B **380**, 7 (1996).

[9] P. Bicudo, Report No. FISIST/5-97/CFIF, hep-ph/9703229, 1997.

[10] P. Bicudo and J. Ribeiro, Phys. Rev. D **42**, 1611 (1990).

[11] Y. le Yaouanc, L. Oliver, S. Ono, O. Pene, and J.-C. Raynal, Phys. Rev. D **29**, 1233 (1984); **31**, 137 (1985).

[12] P. Bicudo and J. Ribeiro, Phys. Rev. D **42**, 1635 (1990); P. Bicudo, J. Ribeiro, and J. Rodrigues, Phys. Rev. C **52**, 2144 (1995); P. Bicudo and J. Ribeiro, *ibid.* **55**, 834 (1997); P. Bicudo, L. Ferreira, C. Placido, and J. Ribeiro, *ibid.* **56**, 670 (1997).

[13] R. Friedrich and H. Reinhardt, Nucl. Phys. **A549**, 406 (1995); S. Gao, C. Shakin, and W.-D. Sun, Phys. Rev. C **53**, 1374 (1996); K. Mitchel and P. Tandy, *ibid.* **55**, 1477 (1997); C. Shakin and W.-D. Sun, Phys. Rev. D **55**, 2874 (1997).

[14] J. E. Ribeiro, Z. Phys. C **5**, 27 (1980).

[15] S. Pepin, F. Stancu, M. Genovese, and J. M. Richard, nucl-th/9608058.

[16] A. Thomas and G. Miller, Phys. Rev. D **43**, 288 (1991).

[17] N. Törnqvist, hep-ph/9612238, 1996; Phys. Lett. B **406**, 70 (1997); **426**, 115 (1998).

[18] P. Bicudo, N. Brambilla, E. Ribeiro, and A. Vairo, Phys. Lett. B **442**, 349 (1998).

[19] M. D' Elia, A. Di Giacomo, and E. Meggiolaro, Phys. Lett. B **408**, 315 (1998).

[20] Y. Kalinowsky, L. Kaslun, and V. Pervushin, Phys. Lett. B **231**, 288 (1989); R. Horvat, D. Kekez, D. Klabucar, and D. Palle, Phys. Rev. D **44**, 1585 (1991).

[21] J. E. Villate, D.-S. Liu, J. E. Ribeiro, and P. Bicudo, Phys. Rev. D **47**, 1145 (1993).

[22] S. Adler and A. C. Davis, Nucl. Phys. **B224**, 469 (1984).

[23] P. Bicudo, G. Krein, J. Ribeiro, and J. Villate, Phys. Rev. D **45**, 1673 (1992).

[24] P. Bicudo and J. Ribeiro, Phys. Rev. D **42**, 1625 (1990).

[25] P. Bicudo, Phys. Rev. Lett. **72**, 1600 (1994).

[26] J. Lagae, Phys. Rev. D **45**, 317 (1992); A. Szczepaniak and E. Swanson, *ibid.* **55**, 3987 (1997).

[27] R. Cahill and C. Roberts, Phys. Rev. D **32**, 2419 (1985).

[28] Y. Dai, Z. Huang, and D. Liu, Phys. Rev. D **43**, 1717 (1991).

[29] Y. Fujiwara and K. T. Hecht, Nucl. Phys. **A451**, 625 (1986).

[30] F. Wang, G. Wu, L. Teng, and T. Goldman, Phys. Rev. Lett. **69**, 2901 (1992); Phys. Rev. C **53**, 1161 (1996).

[31] P. Geiger and N. Isgur, Phys. Rev. D **44**, 799 (1991); Phys. Rev. Lett. **67**, 1066 (1991); Phys. Rev. D **47**, 5050 (1993).

[32] J. Schrieffer, *Theory of Superconductivity* (Bemjamin, New York, 1964).

[33] H. Pagels, Phys. Rev. D **14**, 2747 (1976).

[34] G. 't Hooft, Phys. Rev. Lett. **37**, 8 (1976); Phys. Rev. D **14**, 3432 (1976); V. Bernard, R. L. Jaffe, and U.-G. Meissner, Nucl. Phys. **B308**, 753 (1988).